ACKNOWLEDGMENTS

I would like to dole out my gratitude in several different directions:

- To TxDOT, for their financial support, design examples, and technical advice.
- To Dr. Jirsa and Dr. Kreger, for their assistance, guidance, cooperation, and , most of all, patience. Without their guidance, my thesis would probably be little more than the synthesis of an antithesis.
- To Dan Grant and Weixiong Chen, for their efforts in educating me in the ways and whereabouts of the lab tools.
- To the technical and administrative staff at the Ferguson Laboratory, for their daily help, cooperation, and pleasant banter.
- To all of my friends and coworkers, for making life an education in itself. There are too many to mention, but they all are very important to me.
- To my parents, my sister, and the rest of my family, for their love, genes, phone calls, and support.
- To anyone who ever taught me anything.
- To God, for all of the above and anything that I might have missed.

Jeff Schmitz
Austin, Texas
August 1995

ABSTRACT

THE EFFECT OF BAR ORIENTATION

ON THE BEHAVIOR OF COLUMN SPLICES

by

Jeffrey Scott Schmitz, M.S.E.

The University of Texas at Austin

SUPERVISOR: James O. Jirsa

Column Splices can either be oriented in a side-by-side configuration or an offset configuration. The purpose of this study is to examine experimentally the behavior of both splice orientations, and to present recommendations for their usage.

Four column specimens were tested and evaluated. Each had a 36-inch x 18-inch cross-section, and the columns were 13 feet tall with both side-by-side and offset splices. In total, eight tests were performed considering the effects of the following variables: splice orientation, spacing between splices, and transverse reinforcement. Splice evaluations were based on bar stresses at failure, crack patterns, and modes of failure.

Test results showed that offset splices consistently had higher bond strengths than side-by-side splices. If a splice is designed assuming an offset orientation but constructed as a side-by-side splice, the bond strength may not be sufficient to develop the yield stress of the bars.

TABLE OF CONTENTS

LIST OF TABLES

LIST OF FIGURES

CHAPTER ONE

In Which an Introduction is Made

1.1 Problem Statement

Even though most reinforced concrete structures are considered to be monolithic, it is not possible to construct a complex structure without some construction joints. At such joints, reinforcement is discontinued for ease of construction, but, by lapping bars, the reinforcement is effectively made continuous. Laps are also used in extremely long members because bars are rolled in 60' maximum lengths. Columns, in particular, often have reinforcement spliced with dowels protruding from the footing or column beneath. Also, if a column is sufficiently tall, splices may be required along the height of the column (shown in Figure 1.1).

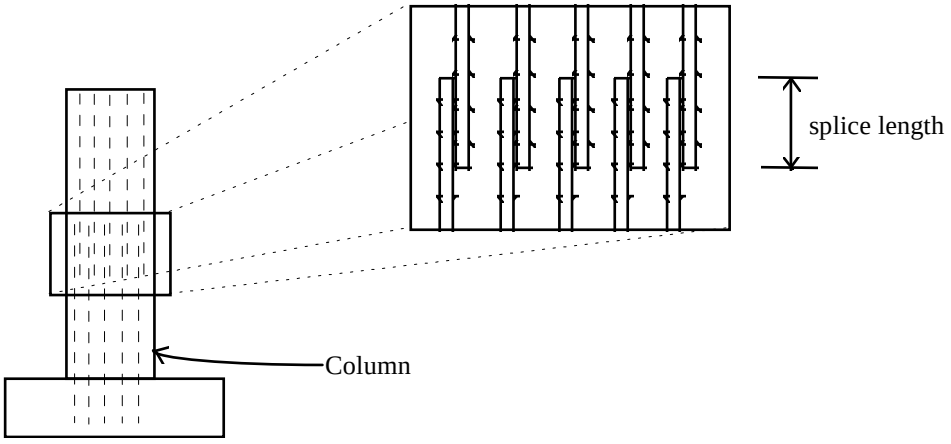

Figure 1.1 Typical lap splices

Column splices can either be oriented in a side-by-side configuration or an offset configuration (see Figure 1.2). The orientation of the spliced bars, whether side-by-side or offset, is not usually specified by the engineer. The splice orientation is chosen by the contractor for ease of fabrication. Side-by-side splices will be more efficient in flexure

than offset splices, with spliced steel distributed farther from the neutral axis near the splice region. Offset splices, though, have more clear spacing between bars, thus reducing the likelihood of a splitting failure in the concrete. Offset splices also offer a construction advantage, enabling the contractror to more easily lower a prefabricated reinforcing cage into place.

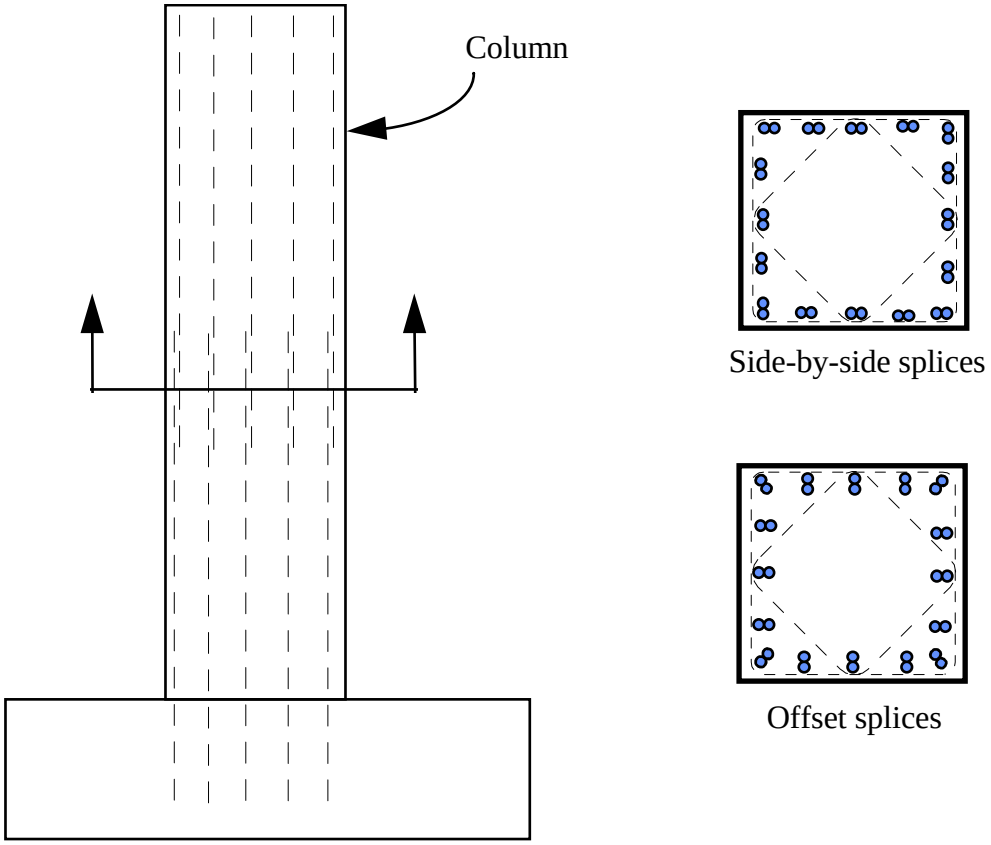

Figure 1.2 Typical splice orientations

The purpose of this study is to examine experimentally the behavior of both splice orientations, and to present recommendations for their usage.

1.2 Project Background

The test program is the final phase of a project, sponsored by the Texas Department of Transportation (TxDOT), in which anchorage and development characteristics of groups of reinforcing bars have been investigated. Previous phases of the project have focused on bundles of reinforcing steel, commonly used in inverse T-beams or bents in highway bridges. Column splices, the focus of this study, are used in footing-to-column shaft connections and, if required, to splice reinforcement along the column's height.

Test specimens were based on TxDOT column details. To accurately assess splice behavior, however, specimens were designed to fail in splitting before the reinforcement yielded. In practice, a splice must be capable of developing sufficiently high stresses, so that failure (splitting) does not occur in the splice. Concrete splitting and bar pullout, the modes of failure for splices of inadequate length, are non-ductile. Ductility is paramount in structural detailing, so that large deformations can be developed prior to failure, and provide a warning that the structure is in distress.

1.3 Object and Scope

The primary objective of this study was to determine the strengths of different splice orientations, side-by-side and offset, as a function of spacing between splices and the presence of transverse reinforcement. Splice behavior was also observed and evaluated based on crack patterns, bar stresses, and mode of failure. The intent is to provide recommendations for the design of splices with varying configurations typical of those used in practice.

Four column specimens were tested and evaluated. Each had a 36-inch x 18-inch cross-section, and the columns were 13 feet tall with both side-by-side and offset splices. In total, eight tests were performed considering the effects of the following variables:

1. Splice orientation, whether side-by-side or offset,
2. Spacing between splices, and
3. Transverse reinforcement.

Other characteristics, such as concrete strength, splice length, bar diameter, and concrete cover, were kept constant for all tests. All testing was performed at the Phil M. Ferguson Structural Engineering Laboratory at the University of Texas at Austin's J. J. Pickle Research Campus.

CHAPTER TWO

In Which a Background is Presented

2.1 The Bond Mechanism

Concrete is reinforced with embedded steel bars where tension is expected to compensate for its low tensile strength. If well designed, an economical, ductile, and versatile building material is produced. Composite action between the concrete and steel depends on bond which allows forces from the concrete to be transferred to the steel. Without bond, the bars would slip, and, to reduce slip of the reinforcement, deformed bars are used.

Originally, plain bars without deformations were used. Bond was developed by chemical adhesion and friction between steel and concrete. The bond from adhesion and friction was easily broken, and anchorage, in the form of hooks or plates, was provided at the end of the bar to prevent the reinforcement from pulling through the concrete [1]. Much of the length of the bars remained unbonded, though, allowing larger deflections and greater crack widths than would occur if the bond was preserved along the entire length. Eventually, reinforcing bars were made with deformations, or lugs, at regular intervals along their lengths to provide mechanical interlock between concrete and steel. Deformed reinforcement improved bond dramatically and is now used almost universally.

The three factors contributing to bond of deformed bars are:

1. Chemical adhesion of the bars to concrete,
2. Friction due to the natural roughness of the bar surface, and
3. Mechanical interlock of the bar deformations with adjacent concrete.

Mechanical interlocking of the lugs is the principal factor contributing to the strain compatibility between concrete and steel. Once adhesion is overcome, it no longer contributes to bond. However, friction may play a significant role, particularly as shown in research where epoxy-coated bars are used [2].

Although bar deformations help to distribute stresses along the bar's length, stress transfer between the concrete and steel is not uniform. Between cracks in the cover, bar

stresses decrease, reflecting the fact that concrete does have some tensile capacity. Average bar stresses are generally used when calculating bond strength. The bond stress can be determined by equating the tension of the bar to the average bond stress over the embedded bar surface. Surface and cross-sectional areas are based on nominal bar diameter, rather than accounting for the increased diameter at deformation locations. The tension force in the reinforcement is then:

$$T = A_b f_s = (\pi d_b) l_s u \qquad (2.1)$$

where: T = tension in the reinforcement

A_b = area of bar, $\pi d_b^2/4$

d_b = bar diameter

f_s = stress in the reinforcement

l_s = anchorage length of the reinforcement considered

u = average bar stress along the anchorage length

Rearranging terms and solving for u,

$$u = \frac{f_s d_b}{4 l_s} \qquad (2.2)$$

The transfer force between the reinforcement and concrete is chiefly developed by the deformations, which, due to their shape, produce a reactive force inclined to the axis of the bar. This inclined force can be expressed as two orthogonal components - one parallel and the other perpendicular to the axis of the bar. While the horizontal component directly resists the bar's tensile force, the perpendicular component acts radially to split the concrete cover and is resisted only by the tensile strength of the surrounding concrete (see Fig. 2.1). Depending on the amount of concrete cover and spacing between bars, the concrete failure can be classified as either a pull-out or a splitting failure. Characterized

by the deformations shearing the surrounding concrete, bar pull-out is likely if the concrete cover and spacing between bars is large. Splitting, however, occurs when bar spacing or concrete cover is small, resulting in spalling of the concrete (see Fig. 2.2).

Figure 2.1 Forces between deformed bars and surrounding concrete [3]

The mode of splitting failure (Fig. 2.3) is determined by the relative sizes of the thickness of face cover (C_b), the thickness of side cover (C_s), and the spacing between bars [3]. Side splitting, characterized by a horizontal split at the level of the bars, occurs when $C_b > C_s$. When $C_s > C_b$, face-and-side splitting occurs, with longitudinal cracking through the bottom cover followed by splitting along the plane of the bars. A V-notch failure - longitudinal cracking followed by inclined cracking through the cover - forms if $C_s >> C_b$.

Figure 2.2 Concrete spalling, the result of splitting

Figure 2.3 Failure patterns for bar splices [3]

2.2 Previous Research

Extensive research has been performed to more fully understand and quantify bond behavior and to provide design recommendations. Because bond failure is a sudden, brittle failure mode, it must be carefully avoided. The guidance provided by research allows engineers to avoid bond failures without providing unreasonably long anchorage lengths.

Previous research indicates that bond strength is dependent on the following factors: concrete tensile strength, bar diameter, thickness of concrete cover, embedment length, casting position, and confinement due to transverse reinforcement. From a series of tests on bond, Orangun, Jirsa, and Breen [3] empirically derived, using a regression analysis, a relationship for bond. They expressed bond as a function of the concrete strength, bar diameter, thickness of concrete cover, embedment, and confinement due to transverse reinforcement. Test results showed that, within certain limits, an increase in bar diameter decreased bond capacity, while an increase in any of the other parameters improved bond performance. Furthermore, Orangun, et al, were able to separate the contributions of plain concrete and transverse reinforcement to bond strength. Their equations for bond strength are applicable to both splices and individual bars being developed. The average bond strength for cases without transverse reinforcement is given by:

$$\frac{u_c}{\sqrt{f'_c}} = 1.2 + 3\frac{C}{d_b} + 50\frac{d_b}{l_s} \qquad (2.3)$$

Test results demonstrated that transverse reinforcement improved anchorage ductility. An increase in the increment of stress over that provided by the concrete cover alone was observed for an increase in the amount of transverse reinforcement. There is, however, an upper limit to the benefit provided by transverse steel. To reflect this situation, the limit of $u_{tr} \Big/ \sqrt{f_c'} \leq 3$ was placed on the contribution of transverse steel to bond strength.

$$\frac{u_{tr}}{\sqrt{f'_c}} = \frac{1}{500}\left(\frac{A_{tr} f_{yt}}{s d_b}\right) \leq 3 \qquad (2.4)$$

For the tests considered by Orangun, et al, bars were immediately adjacent to transverse reinforcement. The effect of confinement on average bond strength may not be as beneficial otherwise. Bars not located at the bend or hook of the transverse steel may not be as effectively restrained.

The total bond strength of a given bar can be taken as the sum of the components due to plain concrete (Equation 2.3) and transverse reinforcement (Equation 2.4).

$$u_{cal} = u_c + u_{tr} \qquad (2.5)$$

$$= \left(1.2 + 3\frac{C}{d_b} + 50\frac{d_b}{l_s} + \frac{A_{tr} f_{yt}}{500 s d_b}\right)\sqrt{f'_c} \qquad (2.6)$$

where: A_{tr} = area of transverse reinforcement crossing the plane of splitting, in^2.

C = the smaller of C_b and C_s, in.

C_b = clear bottom cover to main reinforcement, psi.

C_s = half clear spacing between bars or splices or half available concrete width per bar of splice resisting splitting in the failure plane, psi.

d_b = diameter of main reinforcement, in.

f_{yt} = yield stress of transverse reinforcement, psi.

f'_c = concrete compressive strength, psi.

l_s = length of lap splice, in.

s = spacing of transverse reinforcement, center-to-center, psi.

u_c = calculated average bond stress - without transverse reinforcement, psi.

u_{tr} = portion of strength contributed by transverse reinforcement, psi.

u_{cal} = calculated average bond stress - with transverse reinforcement, psi.

Equations 2.3 through 2.6 can be modified to reflect the lessened bond strength due to top-cast effects. If there is more than 30 cm (12 in.) of concrete cast below the reinforcement in question, the bond strength given in equations 2.3 through 2.6 should be reduced by a factor of 1.3.

It is more important, practically speaking, to determine a required splice length than an average bond stress. By setting equations 2.1 and 2.5 equal to each other, an estimate of the required splice or development length can be made:

$$l_s = \frac{\left(d_b \frac{f_s}{4\sqrt{f'_c}} - 50 \right)}{\left(1.2 + 3\frac{C}{d_b} + \frac{A_{tr} f_{yt}}{500 s d_b} \right)} \qquad (2.7)$$

The yield stress of the steel being developed or spliced would be substituted for f_s to provide sufficient anchorage.

2.3 Current Code Provisions

In the 1995 ACI Building Code Requirements for Reinforced Concrete, a required development length is determined by using one of two sets of equations [4,5]. The first set of equations are a simplified approach for which the contribution of transverse steel is considered to be constant for all cases. Required development length, expressed in terms of the diameter of the bars being developed, is a function of the yield strength of the steel, the concrete compressive strength, and factors to reflect the effects of lightweight aggregate, epoxy coating, and bar location. These equations were developed to expedite the design process, recognizing that many practical construction cases utilize certain combinations of transverse reinforcement and bar spacing. The simplified equations are presented in Table 2.1.

(2.8), (2.9)

(2.10), (2.11)

Table 2.1 Simplified equations from ACI 318-95

ACI also presents an equation similar in form to Equation 2.7 that more accurately considers the effect of transverse reinforcement on bond strength. This equation is applicable for all cases, regardless of bar size, bar spacing, or presence of transverse reinforcement. Similar to the simplified equations, the required development length is expressed in terms of the diameter of the bars being developed. Unlike the simplified equations, though, a designer could consider the effects of specific combinations of cover, spacing, and transverse reinforcement. This more generalized equation is:

$$\frac{l_d}{d_b} = \frac{3}{40}\frac{f_y}{\sqrt{f'_c}}\frac{\alpha\beta\lambda\gamma}{\left(\frac{c + K_{tr}}{d_b}\right)} \qquad (2.12)$$

where $\frac{c + K_{tr}}{d_b}$ shall not be taken greater than 2.5.

The variables for all of the ACI equations presented above are defined as follows:

l_d = required development length, in.

d_b = diameter of bars being spliced, in.

f_y = yield strength of steel, psi.

f'_c = concrete compressive strength, psi.

c = minimum of the thickness of face cover or half the clear spacing between adjacent splices, in.

$$K_{tr} = \frac{A_{tr} f_{yt}}{1500sn}$$

where A_{tr} = total cross-sectional area of all transverse reinforcement which is within the spacing s and which crosses the potential plane of splitting, in^2.

f_{yt} = yield strength of transverse reinforcement, psi.

s = maximum spacing of transverse reinforcement within l_d, in.

n = number of bars being developed along the plane of splitting.

α = bar location factor

β = coating factor

γ = bar size factor

λ = lightweight aggregate concrete factor.

The American Association of State Highway and Transportation Officials (AASHTO) has also published specifications on the design and construction of concrete structures. In the current AASHTO provisions [6], a required development length is determined in a multipartite process. A basic development length, l_{db}, is first calculated based upon the concrete compressive strength and the size and yield strength of the bars being spliced. Factors can then be applied to that basic development length to adjust the required splice length to suit the conditions. Factors are dependent on cover, spacing between splices, transverse reinforcement, top casting, epoxy coating, lightweight aggregate, and excess reinforcement. The development length is:

$$l_d = \left(\frac{1.25 A_b f_y}{\sqrt{f'_c}} \right) \times F_{mod} \qquad (2.13)$$

but not less than

$$l_d = \left(0.4 d_b f_y \right) \times F_{mod} \qquad (2.14)$$

The variables for the AASHTO equation presented above are as follows:

l_d = required development length, in.

A_b = cross-sectional area of the bar being developed, in^2.

f_y = yield strength of bar being developed, ksi.

f'_c = compressive strength of concrete, ksi.

F_{mod} = product of all applicable modification factors.

All ACI- or AASHTO- calculated development lengths are further factored for splices. Depending on the number of bars spliced at a certain location and the ratio of the amount of reinforcement provided to the amount required by analysis, a splice is classified accordingly. A factor is then applied to the development length, based on the splice classification. No splice length shall be less than 12 inches.

CHAPTER THREE

In Which the Experimental Program is Described

3.1 Introduction

Four specimens were constructed with longitudinal steel on one side spliced in a side-by-side configuration and an equal number of offset splices on the opposite side. The two sides were tested separately and consecutively so that eight configurations were tested.

During each test, data were collected until splice failure was reached. At failure, there was a sudden and severe loss of capacity, accompanied by splitting in the concrete cover. The concrete cover in the splice region was removed so that the failure plane could be examined.

3.2 Variables

Earlier research indicated a relationship between splice strength and numerous factors, including: concrete strength, clear spacing between splices, concrete cover, bar diameter, splice length, casting position, and confinement by transverse reinforcement. In this study, concrete strength, cover, bar diameter, splice length, and casting position were kept constant, while the effects of splice configuration, splice spacing, and confinement by transverse reinforcement were examined. For easy reference, tests are denoted by three labels in the following format.

N-C-S

where N = number of splices, 9 or 12
C = splice configuration, O (for offset) or S (for side-by-side)
S = transverse steel, P (for present) or A (for absent)

3.2.1 Splice configuration

Bars were either spliced in an offset configuration or side-by-side. Each specimen had offset splices along one face and an equal number of side-by-side splices along the opposite face. The difference between the two configurations is most clearly manifest in the clear spacing between splices (shown in Figure 3.1) and the effective depth of the steel with respect to the compression face.

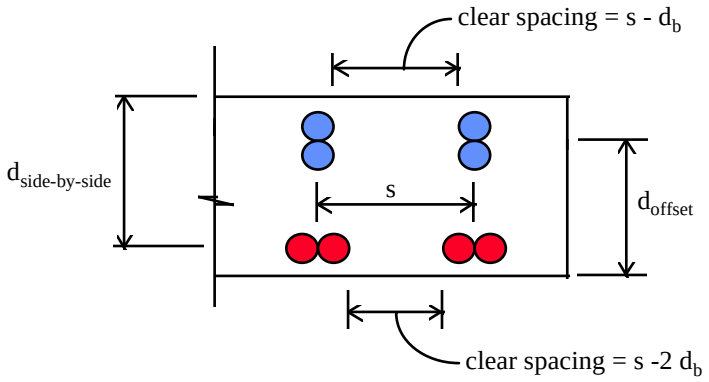

Figure 3.1 Clear spacing between splices

3.2.2 Splice spacing

The center-to-center spacing between splices was uniform within each specimen but was varied between specimens. Clear spacing is determined by splice orientation. Offset splices have a clear spacing one bar diameter larger than their side-by-side counterparts.

3.2.3 Configuration of transverse reinforcement

Complementary tests, some with and others without transverse reinforcement, were devised to demonstrate the effects of confinement.

3.3 Specimen Design

A Texas Department of Transportation (TxDOT) column design (shown in Fig. 3.2) used for the Houston Ship Channel served as an initial model for the column test specimens. Its 36-mm diameter (#11) longitudinal steel was lap spliced with dowels protruding from the footing. Since the loads required to test the massively proportioned column would exceed the capacity of Ferguson Structural Engineering Laboratory's test floor, a half scale specimen was used.

Each specimen was 91 cm (36 in.) x 46 cm (18 in.) x 4 m (13 feet) tall. The longitudinal steel, 19-mm diameter (#6) bars, was spaced along the 91-cm (36-in.)-wide faces and spliced at mid-height, with offset splices on one side and side-by-side splices on the other. Spaced at 13 cm (5 in.) on center, 10-mm diameter (#3) stirrups were used outside the splice region of every specimen. Not all specimens, however, utilized transverse reinforcement in the splice region. The clear concrete cover over the stirrups was 3 cm (1¼ in.).

To accurately observe the behavior and failure of splices, it is important to prevent yielding of the steel being spliced. The ACI equation shown in Table 2.1 estimates that a splice length of 83 cm (33 in.) would be required to fully develop 414-kPa (Grade 60), #6 bars with 20.7-kPa (3,000-psi) concrete. The AASHTO specifications require a splice length of 49 cm (19 in.) to develop the splice with the given conditions. The splice length used for all specimens was 30.5 cm (12 in.), ensuring that, before the longitudinal steel could yield, the splice would fail due to splitting of the concrete.

Although columns, in general, resist both axial load and bending moment, no axial load was applied to the specimens. Bar stresses at the splice are not dependent on loading conditions. Strain gages were placed 30.5 centimeters (12 inches) from the spliced end of bars to measure the steel strain. Both bars of three splices were gaged for each test.

The test set-up, shown in Figure 3.3, was a third-point loading configuration. A constant bending moment, with no shear, was developed between supports. After one side of the specimen was tested, it was turned over so that the second test could be performed. Although cracking from the first test was expected to affect the loading of the second side, it should not have seriously affected the splice strength of the second test. At the completion of the second test, the concrete cover over the splice region was removed to allow inspection of the failure plane. Finally, the specimen was again turned over, and the cover was removed to examine the splice that was tested first. The properties and test conditions for each specimen are shown in Table 3.1.

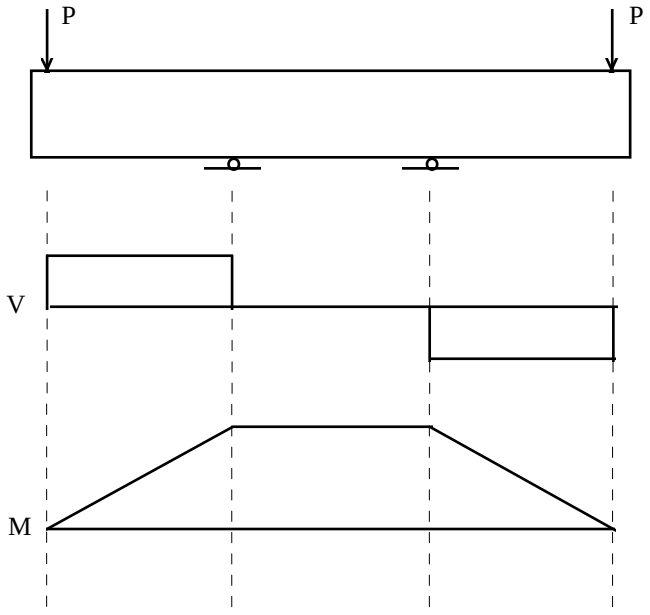

Figure 3.3 Loading Configuration

3.3.1 Specimen #1 (Tests 12-S-P and 12-O-P)

The first specimen had twelve splices of each configuration, with transverse steel confining the splice region. The actual concrete cover over the longitudinal bars was 4 cm (1.75 in.) for the side-by-side splices and 5 cm (1.875 in.) for the offset splices. Offset splices were evaluated in Test 12-O-P, while in 12-S-P side-by-side splices were tested. A cross-section through the splice region is shown in Figure 3.4.

3.3.2 Specimen #2 (Tests 9-S-P and 9-O-P)

Only nine splices of each configuration were used in the second specimen, and transverse steel confined the splices. The side-by-side splices were tested in 9-S-P, and in Test 9-O-P, the performance of the offset splices was evaluated.

The actual concrete cover varied over the width of the specimen. At the specimen's center, there was 10 cm (3¾ in.) of cover over the side-by-side splices and 4 cm (1½ in.) over the offset splices, while, near the edges of the specimen, the cover was 8 cm (3.125 in.) over the side-by-side bars and 3 cm (1¼ in.) over the offset bars. The discrepancy in the concrete cover was the result of inadequate bracing of formwork during placement. Figure 3.5 shows the splice region cross-section.

3.3.3 Specimen #3 (Tests 12-O-A and 12-S-A)

Specimen #3 had twelve side-by-side splices, twelve offset splices, and no transverse steel in the splice region. The two tests performed were used to evaluate the behavior of side-by-side splices (12-S-A) and offset splices (12-O-A), respectively. Five cm (2.125 in.) of concrete covered the side-by-side splices, while the offset splices were covered by 4 cm (1½ in.) of concrete. Figure 3.6 depicts Specimen #3's actual cross-section.

3.3.4 Specimen #4 (Tests 9-O-A and 9-S-A)

The fourth specimen had nine splices of each configuration, with no transverse steel to confine the splice region. The actual concrete cover was 3 cm (1.375 in.) over the offset splices and 5 cm (2 in.) over the side-by-side splices. The offset splices were tested in Test 9-O-A and side-by-side splices were tested in 9-S-A. A cross-section through the splice region is shown in Figure 3.7.

3.4 Materials

3.4.1 Concrete

To ensure a splitting failure prior to yielding of the splices, a low concrete strength was chosen. The 28-day, nominal strength was 0.021 MPa (3,000 psi), but the actual cylinder strengths ranged from 0.019 MPa (2,760 psi) to 0.03 MPa (4350 psi). Because spacing between the steel reinforcement and formwork was tight, and because of difficulty in thoroughly vibrating the bottom of the column, a high slump mix with 9.5-mm (0.38 in.) coarse aggregate was chosen to improve consolidation.

During placement, a crane lifted a concrete bucket to the top of the column, where it was placed in approximately 60-cm (2-foot) lifts using a tremie to funnel the fresh concrete between the stirrup legs of the reinforcement cage.

Cylinder strengths were measured at prescribed intervals. A typical strength-gain curve is shown in Figure 3.8.

3.4.2 Reinforcement

All reinforcement was from the same heat. Longitudinal steel was #6 bars and the transverse reinforcement was #3 bars. The nominal yield stress was 0.41 MPa (60 ksi), but

tests revealed that the actual yield stress was 435 MPa (63 ksi) for the longitudinal steel and 440 MPa (64 ksi) for transverse reinforcement.

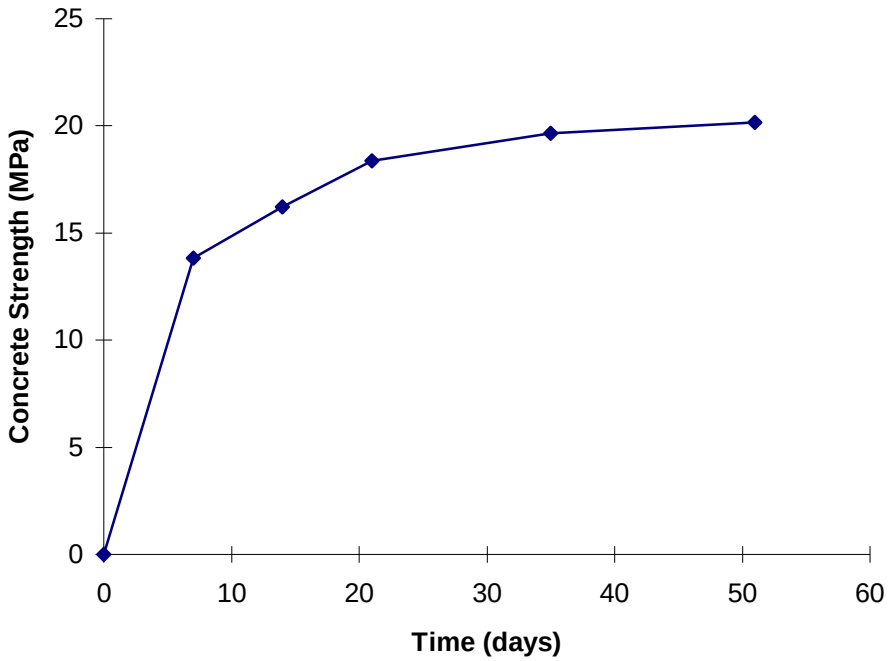

Figure 3.8 Typical concrete strength curve

3.5 Specimen Construction

The reinforcement cage was constructed in a horizontal position using three sawhorses: one on each end and one in the middle. First, the side-by-side splices were arranged as the bottom layer of longitudinal steel. The stirrups were then placed. Since four stirrup legs were needed every 13 cm (5 in.) along the column's height, two stirrups were placed at each location. The transverse steel was tied so that the bars spliced side-by-side were at the bottom of the stirrups. Finally, the offset splices were tied at the top of, but still inside, the stirrups.

All strain gages were placed prior to cage construction. After the reinforcement cage was completed, the strain gage lead wires were gathered to exit the column at one location. Figure 3.9 is a photo of a fabricated reinforcing cage.

Figure 3.9 Photograph of a fabricated reinforcing cage

Formwork was assembled with three sides attached to each other and standing upright. After the reinforcement cage was placed upright into the formwork, as shown in Figure 3.10, the fourth side was attached. For convenient transport of the specimen, threaded inserts were cast into each column.

3.6 Loading System

The column rested horizontally on two supports, spaced 1.2 m (4 feet) apart and centered under the specimen. Both supports were rollers, allowing the specimen to rotate

Figure 3.10 Position of reinforcing cage prior to casting

and translate freely. Load was applied to each end of the column through loading beams placed on the specimen 1.2 m (4 feet) from the supports. Two, 534-kN (60-ton) capacity rams loaded each loading beam, with the load being transferred to the floor by four threaded rods per ram. One pump activated all four rams. The test set-up is shown in Figures 3.11, 3.12, and 3.13.

Figure 3.11 Photograph of test set-up

3.7 Testing Procedure

Loads were applied incrementally and data were recorded at 11-kN (2.5-kip) intervals. The appearance of both the first crack and the first crack in the splice region was noted. At each load step, the crack progress was monitored and the shape was traced on the

specimen. When splitting occurred, data were recorded. Data were recorded as the load on the specimen was decreased to zero.

After failure and removal of the load, all deflection indicators were removed. Then, the ends of the specimen were further displaced until the concrete cover over the splice could be easily removed. No data were recorded during this stage of testing.

3.8 Strain and Deflection Instrumentation

Stresses in the reinforcement were calculated from strains recorded during testing. These strains were measured by gages placed in strategic locations in the splice region. For each instrumented splice, a gage was placed on each bar, 30.5 centimeters (12 inches) from the spliced end. The first, third, and fifth splices from the edge were instrumented for tests with nine splices, while for tests with twelve splices, the first, fourth, and fifth splices were gaged. In every case, two splices were in the corner of a stirrup and one was not. If transverse reinforcement was included in the splice region, all three stirrups were instrumented. All strain gage locations are shown in Figures 3.14, 3.15, and 3.16.

Linear potentiometers were used to measure deflections. Two linear pots were positioned at each end, and two were used at midspan of the specimen.

CHAPTER FOUR

In Which Results are Displayed

4.1 Introduction

Crack patterns, load-deflection, and load-stress plots are presented for the eight tests performed. To aid in understanding, certain key terms used in the discussion are defined in Figure 4.1. The results of each test are described in the order in which the tests were performed.

4.2 Tests With Transverse Reinforcement

Four tests were performed in which transverse reinforcement crossed the expected failure plane. For each test including transverse steel, ties were located at three locations in the splice region. The transverse steel was spaced along the splice at 13 cm (5 in.), on center.

There were twelve “active” strain gages on the stirrups for each of the tests. Six of the gages were located on the tie legs to measure strain induced by splitting along the layer of longitudinal reinforcement. The other six gages were placed to measure the strain caused by longitudinal cracking along the splice in the concrete cover. The instrumentation for the transverse reinforcement is described in Figure 4.2.

All deflections refer to measurements at the ends of the specimens. The average of four deflection readings, two at each end, was used in the load-deflection plots. Recorded midspan deflections are not included in presenting load-deflection relationships because they were small and consistent with end deflection readings.

4.2.1 Test 12-S-P

The behavior of twelve splices, arranged in a side-by-side configuration, was examined in test 12-S-P. Clear spacing between splices was 4 cm (1.38 in.) - the equivalent of 1.83 bar diameters. Although the specimen was designed to have a clear face cover of 4.1 cm (1.63 in.), the actual face cover was 4.5 cm (1.75 in.). 12-S-P was the first test performed on Specimen #1.

The load-deflection plot (see Figure 4.3) shows a noticeable decrease in stiffness after first cracking. After that first change in stiffness, the stiffness was essentially constant until failure. At failure, there was increased deflection without additional load, and as load was removed, deflections decreased. After all loads were removed, there was a permanent deflection of the specimen.

The stress was essentially uniform for all longitudinal bars during testing. The load-stress plot (see Figure 4.4) for longitudinal reinforcement is similar to the load-deflection plot, with a decreasing slope as the specimen approached failure. The plot is almost bilinear, with a change in slope at a stress of about 40 MPa (5 ksi). The load at failure was 209 kN (47 kips), corresponding to a bar stress of about 200 MPa (30 ksi). A straight-line prediction of the load vs. stress relationship, based on a cracked section analysis, is also shown in Figure 4.4. As cracking progresses across the section and more flexural cracks form, bar stresses closely match the failure stresses predicted by straight-line theory, reinforcing the validity of the cracked section analysis.

The strain gages on the transverse tie legs that monitored splitting indicated very low strains until face splitting occurred. At failure, though, some stirrups indicated compression while others indicated tension. The gages on the lateral tie legs, on the other hand, registered stress at a lower load and, at failure, measured only tensile stresses. Tie stresses are shown in Figures 4.5 and 4.6. The location of splitting cracks relative to the location of strain gages probably accounts for the development of compressive strains in some bars and erratic behavior in others.

Failure occurred at a load of about 220 kN (50 kips). Transverse face cracking occurred prior to failure, most noticeably over the tie locations. After splitting occurred, there were severe cracks , both longitudinal and transverse, throughout the splice region, with cracks in the side cover at the level of the longitudinal reinforcement. Crack patterns are shown in Figure 4.7. The face cover, after splitting, was loose, separated from the specimen by a failure plane passing though the plane of the splices, as shown in Figure 4.8. The failure itself was sudden, but not violent, and the cover, though split from the specimen, was still attached to the stirrups.

4.2.2 Test 12-O-P

Test 12-O-P is the complement of 12-S-P in that both were on the same test specimen, but the splices were oriented in an offset configuration with a clear spacing of 5 cm (2.125 in.) - the equivalent of 2.83 bar diameters. 12-O-P was the second test of Specimen #1. The face cover was 4.76 cm (1.875 in.) over the offset splices.

The load-deflection plot (see Figure 4.9), when compared to that of 12-S-P, is initially very flat. That low stiffness reflects the fact that very little load was required to close the cracks formed during 12-S-P, but after those cracks closed, the stiffness increased drastically. Eventually, new cracks formed over the offset splices, and, similar to the behavior of Test 12-S-P, the stiffness decreased and then remained constant until the peak load was reached. After the load was completely removed, there was permanent deflection. The permanent deflection of 12-O-P was much larger than that of 12-S-P, primarily due to the damage to the section as large deformations were applied. The dashed line in Figure 4.9 represents the estimated path that the load-deflection plot would have taken if 12-O-P had been the first test performed on Specimen #1.

The bar stresses for the splices of 12-O-P did not behave as uniformly as those of 12-S-P. The bars nearest to the face (or outside bars) had a higher stress than the bars away from the concrete face. All splices failed at the same peak load with bar stresses

ranging from 152 MPa (22 ksi) for the inside bars to 202 MPa (29 ksi) for the outside bars. The peak load was about 210 kN (47 kips). The inconsistency of the stress readings is believed to be the result of cracking from Test 12-S-P, previous to 12-O-P. The load-stress plot is shown in Figure 4.10a. A segment of each gage reading has a constant slope that is similar to the slope of the straight-line prediction from the cracked section analysis. The straight portions of the plots begin when the cracks of 12-S-P have completely closed. The constant slopes are extrapolated to the axis of zero load to estimate how the splices would have behaved if the cracks from 12-S-P had been closed prior to the testing of 12-O-P.

Figure 4.10b shows the complete adjustment of the measured bar stresses. The zero-load point of each plot is shifted to the origin, corresponding to zero stress. The slopes of the adjusted plots are similar to the straight-line predictions from a cracked section analysis.

Most of the gages on the lateral tie legs of the transverse reinforcement detected almost no strain. One gage slightly increased in strain as the load increased. At failure, the stress in all of the stirrups suddenly increased drastically, reflecting longitudinal cracking in the face cover at failure (see Figure 4.11). Only two of the gages on the lateral tie legs, on the other hand, drastically increased in stress at failure (see Figure 4.12). The rest of the gages remained virtually unstrained through the duration of the test.

Transverse cracking over the stirrup locations was the first cracking noticed. Those cracks increased in both length and width until failure. When splitting occurred, the concrete face cover cracked both longitudinally and diagonally over the splice, and the side cover cracked at the level of the splices. Crack patterns can be seen in Figure 4.13. The failure plane passed between the inside and outside spliced bars, as if the outside bars simply pried the cover above them off, leaving the concrete below unaffected (see Figure 4.14). Outside the splice region, the cover remained intact.

4.2.3 Test 9-S-P

In this test, there were 9 splices, confined by transverse reinforcement and arranged in a side-by-side configuration. The clear spacing between adjacent splices was 6 cm (2.44 in.), and the clear face cover over the splices was 9 cm (3.75 in.) at the specimen's center and 7 cm (3.125 in.) at the edges. 9-S-P was the first test of Specimen #2.

Similar to that of Test 12-S-P, the load-deflection plot (shown in Figure 4.15) is practically bilinear. The specimen became less stiff after the first crack, at a load of about 75 kN (17 kips). The peak recorded load was 182 kN (41 kips), after which the deflection increased with no load increase and then decreased as the load was removed. The permanent end deflection of 9-S-P was about 0.5 cm (0.2 in.).

From the load-stress plot shown in Figure 4.16, it is evident that bar stress was not uniform for all splices. The two strain gages on any particular splice were 31 cm (12 in.) apart since gages were only placed at the edge of the splice region. The three gages located on one side of the splice region behaved similarly, while the other three gages behaved similarly to each other, but differently than the first three gages. Although the two groups of gages were strained differently throughout most of the test, both sides of the splice region were stressed similarly at failure. The average stress calculated from the strain gages closely matches the predicted stresses at failure, as shown in Figure 4.16.

The transverse reinforcement remained virtually unstressed until splitting occurred. The lateral legs of the instrumented ties were nearly all in tension at failure (see Figure 4.17). The transverse tie leg stresses, on the other hand, were more varied. The recorded stresses for the vertical legs ranged from more than 65 MPa (10 ksi) in compression to more than 140 MPa (20 ksi) in tension (see Figure 4.18).

Prior to failure at a peak load of 182 kN (41 kips), there was transverse cracking in the face cover over the stirrup locations. Those transverse cracks widened at failure, accompanied by the formation of longitudinal cracks in the side cover at the level of the splices. No longitudinal cracks developed in the face cover. Crack patterns can be seen in

Figure 4.19. Probably because of the excessive thickness of the face cover, the splices failed only through side splitting, with the failure plane passing through the level of the splices. The post-failure plane of splitting is shown in Figure 4.20.

4.2.4 Test 9-O-P

For Test 9-O-P, the second test of Specimen #2, there were nine splices with offset configurations and confined by transverse reinforcement. There was 8 cm (3.188 in.) of clear spacing between adjacent splices. The clear face cover over the splices varied from 3.81 cm (1.5 in.) at the center of the specimen to 3.18 cm (1.25 in.) at the edges. In addition, there was severe honeycombing of the concrete face cover just outside the splice region, as shown in Figure 4.21. The honeycombing partially extended, though much less severely, into the splice region. It appears that the honeycombing in the face cover did not adversely affect bond performance, and, after the cover was removed, it could be seen that the concrete damage was superficial and did not reach the level of the splices.

The measured load-deflection relationship (see Figure 4.22) has an increasing slope at low loads. The increasing specimen stiffness is due to the closure of cracks formed during Test 9-S-P. After those cracks closed, the stiffness remained constant until the peak load was reached. The dashed line in Figure 4.22 is an estimation of the path that the load-deflection plot would have taken if the cracks had been closed prior to loading.

The splice stresses varied widely at every load increment (see Figure 4.23a). In this case, bars nearest to the face were not stressed. The bars farthest from the face were also not stressed uniformly. However, the difference in stress between inside and outside bars was similar. Also, just prior to failure, the bars of the splice nearest the edge decreased in tension, perhaps due to the beginning of side splitting. The stresses in the other instrumented longitudinal bars increased up to failure. The differences in the measured stresses is believed to be due to previous cracking of Test 9-S-P. As those cracks closed at the beginning of testing, the bar stresses increased at markedly different rates.

After the cracks had completely closed, though, the slope of each load-stress plot was essentially constant until failure. In Figure 4.23a, the constant slopes are extended to the axis of zero load to estimate how the splices would have behaved if the cracks of 9-S-P had been closed before the testing of 9-O-P. The constant-slope estimations of splice behavior are shifted to begin at zero bar stress in Figure 4.23b. The slopes of the adjusted plots are similar to the slopes of the straight-line predictions made from a cracked section analysis.

The lateral legs of some instrumented stirrups started to increase in stress at a load of about 98 kN (22 kips), while others remained unstressed until failure, at a peak load of about 222 kN (50 kips) (see Figure 4.24). The three gages that registered stress at the lower loads were all near the edge of the specimen and probably due to the formation of a longitudinal crack near that splice.

The transverse tie legs were also stressed before the peak load was reached. The vertical legs, though, were inconsistently stressed - some in tension and others in compression (see Figure 4.25).

Failure for 9-O-P was reflected by both longitudinal and transverse cracking in the face cover and by cracking in the side cover at the level of the splices (see Figure 4.26). The splitting plane passed horizontally between any two bars spliced together (see Figure 4.27).

4.2.5 Interaction between spliced bars and ties

When ties are present in the splice region, any cracking due to splice failure is resisted by the ties crossing the failure plane. The stresses in the spliced bars and the ties should reflect this interaction. Figures 4.28 and 4.29, the load-stress plots for splices and ties of Test 9-S-P, demonstrate the relationship between ties and splices as splice failure occurs.

The enervation of a splice, manifested as an increase in slope on the load-stress plot, occurs when splitting or micro-cracking begins near the splice. If the splice is

immediately adjacent to a transverse tie leg, the weakening of the splice should be accompanied by an increase in stress in the tie. Figures 4.28 and 4.29 demonstrate this; for any increase in slope of the load-stress plot of the spliced bars, there is a corresponding and simultaneous increase in stress for some of the tie legs. At failure, as the splices lose stress and the splitting plane widens, the transverse steel increases in stress dramatically.

4.3 Tests Without Transverse Reinforcement

Four tests were performed in which transverse reinforcement was omitted from the splice region. The ACI and AASHTO specifications allow shorter lap splices if there is adequate confinement from transverse reinforcement. Stirrups, though, are not required where bars are spliced, unless required for other concerns. Therefore, some splices were not confined by stirrups to help determine the effect of transverse reinforcement on splice behavior.

4.3.1 Test 12-O-A

The behavior of twelve splices, each with an offset configuration, was examined in Test 12-O-A, the first test of Specimen #3. The clear face cover over the splices was 3.81 cm (1.5 in.) across the specimen, just as intended in design, and clear spacing between splices was 5 cm (2.125 in.).

As shown in the load-deflection plot for 12-O-A (see Figure 4.30), the specimen was initially very stiff, becoming less so after first cracking. After cracking had occurred, the slope of the load-deflection plot decreased but thereafter remained constant until a peak load of 265 kN (60 kips) was reached. The sustained load decreased sharply at failure, accompanied by large deflections. The uncertainty of the exact path at failure is reflected by a dashed line in Figure 4.30. As the load was completely removed, the defection slightly decreased. A permanent deflection of about 0.9 cm (0.35 in.) was recorded.

The instrumented splices indicate that the bars closest to the concrete face were less stressed than the inside bars, as expected. The inner bars have a shorter moment arm than the outside bars, thus needing to carry a larger force to produce an equal moment. As the bars approached failure, stresses in the outer bars began to deviate from each other, and the inner bars performed likewise. At failure, the stresses calculated from measured strains approached predicted stresses calculated from the cracked section analysis. After the peak load was reached, the bar stresses immediately dropped off sharply as the splices could sustain no more load. Figure 4.31 shows the load-stress plot.

The cracking before failure consisted mostly of transverse cracks in the face cover at the borders of the splice region. Failure was very sudden and definite, with the load-dropping nearly to zero. Inclined cracks appeared in the side cover at the level of the splices, and some diagonal and longitudinal cracks joined the widened transverse cracks in the face cover (see Figure 4.32). The face cover over the splices did not completely separate from the rest of the specimen, although the face and side cover along the edges did spall off, as shown in Figure 4.33.

4.3.2 Test 12-S-A

In Test 12-S-A, the second test of Specimen #3, twelve splices were oriented in a side-by-side configuration. The clear cover over the spacing, although designed to be only 4 cm (1.625 in.), was actually 5.4 cm (2.13 in.) as constructed. Clear spacing between adjacent splices was 4 cm (1.38 in.).

The specimen initially had increasing stiffness after the first load step of 12 kN (2.7 kips) (see Figure 4.34). The increasing stiffness is due to the closing of cracks from Test 12-O-A, which was performed prior to 12-S-A. After the effects of prior cracking were overcome, the specimen had an essentially constant stiffness until failure. An approximation of the initial path that would have been taken if Test 12-S-P had been performed first is shown as a dashed line in Figure 4.34. At the peak load of 201 kN (45

kips), the deflection suddenly increased drastically, as the specimen's load carrying capacity dropped severely. The exact load-deflection behavior is unknown, and the uncertainty is reflected on the plot. The applied load was then removed, leaving a permanent deflection of the specimen's ends.

The bars all increased in stress uniformly, following the same path on the load-stress plot (see Figure 4.35a). Surprisingly, the bars initially all went into compression until, at a load of approximately 65 kN (15 kips), they were in tension. The initial compression measured in the splices is believed to be the result of the previous cracking from Test 12-O-A. After the cracks of 12-O-A were closed, the bar stress increased at a constant rate with respect to load until the peak load was reached. At failure, the stress in two instrumented bars was lost completely, while the other bars only partly lost their peak stress. An estimation of how the splices would have behaved if the 12-O-A cracking had been closed prior to testing can be made by extending the constant slope of the plot to the axis of zero load. That estimation is shown as a dashed line in Figure 4.35a. In Figure 4.35b, the estimated load-stress path is shifted so that, at the onset of loading, there is no stress in the splices. The path of the adjusted load-stress plot correlates closely with the prediction made by using a cracked section analysis.

Splitting caused transverse and diagonal cracks in the splice region's face cover and longitudinal cracks in the side cover at the level of the splices (see Figure 4.36). There was no longitudinal cracking in the face cover. The entire face cover and a portion of the side cover was loose after splitting and could be easily removed, showing that the failure plane passed through the plane of the spliced bars (shown in Figure 4.37).

4.3.3 Test 9-O-A

The nine splices of Test 9-O-A, the first test of Specimen #4, were in an offset configuration with 8 cm (3.18 in.) of clear spacing between adjacent splices. The clear face cover over the offset splices was 3.49 cm (1.375 in.)

The load-deflection plot (see Figure 4.38) shows that the specimen was initially very stiff, decreasing in stiffness only after cracking occurred. A peak load of approximately 265 kN (60 kips) was reached. After failure, deflections continued to increase without additional load. The exact path of the load-deflection plot at failure is unknown; an estimation is shown as a dashed line in Figure 4.38. A permanent deflection of about 0.85 cm (0.33 in.) was recorded after the load was completely removed.

The instrumented bars were all at the same level of stress until they reached a stress of about 20 MPa (2.5 ksi). At that point, each bar's load-stress plot suddenly changed slope and their paths diverged. The outside bars, as expected, had a lower average stress than the inside bars because of their larger moment arm When the peak load was reached, the load abruptly decreased. For splices with one bar more highly stressed than the other, the bar with higher stress prior to failure had less stress than the other bar afterwards as stress was transferred between bars. A peak load of 226 kN (51 kips) was reached. The bar stress at failure, as indicated by strain gage data, approached the predictions made using the cracked section analysis. The load-stress plot is shown in Figure 4.39.

There was both longitudinal and transverse cracking in the face cover at failure, and the side cover cracked both vertically and diagonally (see Figure 4.40). There was no purely longitudinal cracking in the side cover. Splitting occurred suddenly, and, when it did, the specimen's load-carrying capacity decreased sharply. The face cover could only be removed near the edges of the splice region (see Figure 4.41); the remaining face cover was not loosened by splitting.

4.3.4 Test 9-S-A

The second test of Specimen #4, 9-S-A, was performed on nine splices arranged in a side-by-side configuration without the confinement of transverse reinforcement. The clear spacing between adjacent splices was 6 cm (2.44 in.), the equivalent of 3.25 bar diameters, and there was 5.08 cm (2 in.) of clear face cover over the side-by-side splices.

Similar to that of Test 12-S-A, the load-deflection plot (see Figure 4.42) initially had an increasing slope after the initial load step, due to the closure of cracks from 9-O-A. When the cracks from previous testing were closed, the slope of the load-deflection plot was constant until failure. A dashed line in Figure 4.42 estimates the path that would have been taken if Test 9-O-A had not been performed prior to 9-S-A. At the attainment of the peak load, deflections increased uncontrollably without an increase in load. The uncertainty of the exact path at failure is reflected as a dashed line in Figure 4.42. The deflections decreased somewhat when the applied load was completely removed.

Prior to failure, the load-stress plot (shown in Figure 4.43a) for each of the spliced bars was almost identical. Similar to the splices of 12-S-A, the bars initially went into compression and gradually were tensioned until failure. The initial compression of the splices is due to cracking from the previous test, 9-O-A. After the previous cracking had closed, the load-stress slopes of the splices was essentially constant until the peak load was reached. The constant slopes can be extended to the axis of zero load, as shown by dashed lines in Figure 4.43a, estimating the load-stress behavior if the 9-S-A cracks had been closed prior to testing. Figure 4.43b shows the adjusted plots shifted so that they begin with no bar stress. The slope of the adjusted plots closely correlates with the straight-line prediction from a cracked section analysis.

There was transverse cracking in the splices' face cover and longitudinal cracking in the side cover at the level of the splices due to splitting (see Figure 4.44). There was never any longitudinal cracking in the face cover during Test 9-S-A. When the face cover was removed, the failure plane could be seen to lie in the plane of the splices, as shown in Figure 4.45.

4.4 Accuracy of Strain Gage Data

The load-stress plots for the splices of each of the tests have both stresses calculated from strain gage data and a straight-line prediction of stresses calculated from a

cracked section analysis of the specimens. For the first tests in a specimen, the paths of the measured and theoretical stresses do not coincide, but they predict approximately the same bar stress near failure when cracks are well developed across the section. For second tests on specimens, the paths of the measured and theoretical stresses match closely after adjustments were made to account for the effects of previous cracking. Generally, the stresses calculated from measured strains and the stresses calculated from loads were close at failure of the splices. In Table 4.1, the calculated failure stresses are summarized and the errors between the two methods of stress calculation are listed. The error for most tests was less than 12%, giving credence to the accuracy of cracked section analysis and explaining the effect of cracking during the first test on the results of the second test.

CHAPTER FIVE

In Which Results are Compared and Discussed

5.1 Introduction

The effects of three parameters - splice orientation, confinement due to transverse reinforcement, and clear spacing between adjacent splices - were investigated in this project. Each specimen was designed to have a unique combination of those three parameters. To best evaluate the effect of a certain parameter, comparisons are made between tests where two parameters are constant while the third parameter varies. For example, to isolate the effect of transverse reinforcement, two tests can be compared where the splice orientation and splice spacing was the same for each test. By comparing the results of several such pairs of tests, general trends in bond behavior become apparent.

Comparisons are partly based on the bar stress at failure. The bar stress used can be either calculated from the loading condition and a cracked section analysis or from the measured bar strain. Table 4.1 showed that the two methods of stress calculation produced reasonably similar stresses at failure. Many of the stresses calculated from measured strains, though, were adjusted graphically to account for the effects of previous cracking. To reduce the uncertainty in the failure stresses, the stresses calculated from loads and a cracked section analysis are used.

For offset splices, the stress at failure can be calculated for both the inside bars and the outside bars. The innermost bar determines when side-splitting occurs, since it has the higher stress. In bond factor comparisons, then, only the stress of the inside bar should be considered. The stress of the outermost bars, because they do not control failure, is not included in the values for the bond strength of offset splices.

The bond factor is the bond stress at failure, with respect to the concrete's tensile strength. Since the tensile strength of the concrete is a major contributor to the bond strength of a bar, the results of specimens with differing concrete strengths can be

normalized by dividing the bond strength by $\sqrt{f_c'}$, a parameter considered to be an index of concrete tensile strength. The experimental bond factor is calculated as follows:

$$\psi_{test} = \frac{u_{test}}{\sqrt{f_c'}} = \frac{f_s d_b}{4 l_s \sqrt{f_c'}} \qquad (5.1)$$

The theoretical bond factor is:

$$\psi_{theory} = \frac{u_{theory}}{\sqrt{f_c'}} = 1.2 + 3\frac{c}{d_b} + \frac{A_{tr} f_{yt}}{500 s d_b} \qquad (5.2)$$

where ψ = bond factor

f_s = bar stress in the splice, psi.

d_b = diameter of bars being spliced, in.

f'_c = concrete compressive strength, psi.

l_s = length of splice, in.

A_{tr} = total cross-sectional area of transverse reinforcement within spacing s and crossing the plane of splitting, in^2

f_{yt} = yield strength of transverse reinforcement, psi.

c = minimum of the thickness of face cover or half the clear spacing between adjacent splices, in.

s = spacing of transverse reinforcement, in.

All bond factor values are displayed in Tables 5.1 and 5.2.

While quantitative comparisons are made using bond factors, qualitative comparisons are also made based on observed crack patterns, failure modes, and other bond behavior.

5.2 The Effect of Splice Orientation

Comparisons of bond factors are made in Table 5.3, where it can be seen that offset splices consistently have higher bond factors than side-by-side splices. Offset splices, due to their orientation, have larger clear spacing between adjacent splices than side-by-side splices. Increased clear spacing between splices has a beneficial effect on bond performance, as shown in Equation 2.6. Thus, if splices fail in side splitting, offset splices have an advantage over their side-by-side counterparts.

Test	ψ_{theory}	ψ_{test}	$\left(\frac{\psi_{offset}}{\psi_{s-b-s}}\right)_{theory}$	$\left(\frac{\psi_{offset}}{\psi_{s-b-s}}\right)_{test}$
12-S-P	8.27	7.85		
12-O-P	9.74	9.07	1.18	1.16
9-S-P	10.77	8.61		
9-O-P	12.30	8.80	1.14	1.02
12-S-A	7.09	6.82		
12-O-A	8.56	9.10	1.21	1.33
9-S-A	9.21	11.08		
9-O-A	10.72	12.35	1.16	1.11
		Averages	1.17	1.16

Table 5.3 Comparison of Splice Orientations

The crack patterns observed for the tests also indicate a difference in the behavior of the two splice configurations. The prime difference was noticed in the crack patterns in the side cover of the specimens. Consistently, side-by-side splices cracked the concrete side cover horizontally, along the level of the splices. Inclined cracks, at an angle of about 45 degrees from the axis of the bars, formed on the side cover for tests involving offset splices. Those inclined cracks always crossed the plane of the splices, inclined in a

direction consistent with the orientation of the spliced bars, as shown in Figure 5.1. The inclined cracks are due to shear generated by the bar forces acting in opposite directions (see Figure 5.2). Side-by-side splices, because of their horizontal plane of alignment, would generate shear in a horizontal plane. The inclined crack formation only occurred between the side face and the outermost splice. Between adjacent splices, the failure plane was always horizontal.

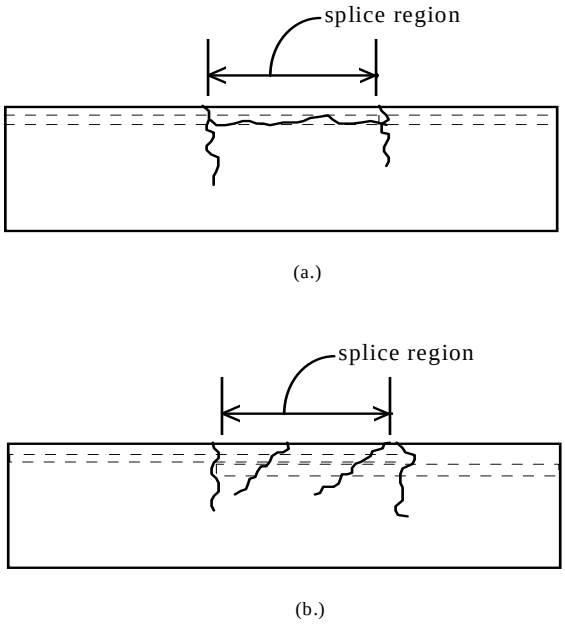

Figure 5.1 Typical crack patterns for (a.) side-by-side splices and (b.) offset splices.

For both side-by-side splices and offset splices, the horizontal plane of splitting passed through the centroid of the splices. For side-by-side splices, the failure plane passed through the center of both spliced bars. The failure plane for offset splices, however, passed between the spliced bars as shown in Figure 5.3. Furthermore, the face cover fully separated from the splices after splitting, except for offset splices in Tests 12-O-A and 9-O-A, where only the cover nearest the sides spalled off.

5.3 The Effect of Transverse Steel

When failure occurred in tests without transverse reinforcement in the splice region, the specimen's ability to sustain load decreased abruptly. The bar stresses for the splices in those tests also suddenly decreased at failure. The sudden failure of the unconfined splices sharply contrasts with the behavior at failure of splices confined by transverse steel. For those tests where stirrups were present, bar stresses could adjust as the peak load was sustained. The strain gage data suggests that, at the same load, some bars decreased in stress while other bar stresses increased. That redistribution of splice stresses only accompanied failure for tests with transverse reinforcement in the splice region. The crack patterns of the failed splices without stirrups differed only slightly from the cracking induced at the failure of splices without stirrups. If stirrups were present, there was transverse cracking in the face cover above each stirrup location. If stirrups were absent from the splice region, there were transverse cracks only at the edges of the splice region. The transverse cracks nearest the edges of the splice region usually progressed vertically down the side cover, regardless of whether transverse reinforcement was absent or present.

For offset splices, only portions of the cover could be removed after failure if there was no transverse steel in the splice region. The remaining cover was still attached to the outside bars because the splitting plane passed between the spliced bars, rather than through both of them. When transverse steel was not present, there was nothing to prevent the face cover from remaining bonded to the outside bars. The failure plane, then, only widened as load continued to be applied, as Figure 5.4 shows. When transverse steel was present, though, the stirrups bound the spliced bars together, preventing them from separating. Splice failure caused the spliced bars to slide against each other, and the radial force of the bars acting on the concrete caused the cover to completely separate from the splices, as Figure 5.5 shows.

Other studies suggest that transverse steel improves bond strength [7]. For the tests in this study, though, the splices confined by transverse steel did not have higher bond factors than splices without transverse steel. The anomaly is likely due to the limited number of tests in this study and the fact that less than half of the splices were immediately adjacent to a transverse tie leg. It is expected that if more tests were performed with better confinement in the splice region, test results would support the trends observed in past studies.

5.4 The Effect of Splice Spacing

Bond factor comparisons, based on splice spacing, are made in Table 5.4. It can be seen that splices in 9-splice tests had 128% of the bond strength of splices in 12-splice tests. This average value very closely matches the theoretical value predicted by using the Orangun, Jirsa, and Breen equation (Equation 2.6). Reduced clear spacing between adjacent splices reduces bond strength if side-splitting is prevalent. The clear spacing for the 12-splice tests was 1.75 cm (0.69 in.) for the side-by-side splices and 3.10 cm (1.22 in.) for the offset splices. The clear spacing for the 9-splice tests, then, increased 77% for the side-by-side splices and 51% for the offset splices. This difference in clear spacing contributes to a lower average bond strength for the more closely spaced splices.

The adverse effect of decreased clear spacing between splices was less severe if transverse steel was confining the splice region. The $\psi_{12\ splices}$ / $\psi_{9\ splices}$ ratio was approximately 39% higher if transverse steel was present. This trend suggests that transverse steel helped to better distribute the bar stresses at failure for tests involving 12 splices. The load vs. bar stress plots for the splices of 12-O-P and 12-O-A demonstrate the advantage of transverse steel. At the failure of Test 12-O-A, the stress in each splice decreased suddenly. In Test 12-O-P, however, failure was more gradual and the peak load could be held. At the peak load, the most highly stressed bars decreased in stress as the stress in the other bars increased. Even though some splices were failing, the confinement provided by the stirrups allowed stress to be transferred to the splices that had not yet failed.

Test	ψ_{theory}	ψ_{test}	$\left(\frac{\psi_{9\ splices}}{\psi_{12\ splices}}\right)_{theory}$	$\left(\frac{\psi_{9\ splices}}{\psi_{12\ splices}}\right)_{test}$
12-S-P	8.27	7.85		
9-S-P	10.77	8.61	1.30	1.10
12-O-P	9.74	9.07		
9-O-P	12.30	8.80	1.26	0.97
12-S-A	7.09	6.82		
9-S-A	9.21	11.08	1.30	1.62
12-O-A	8.56	9.10		
9-O-A	10.72	12.35	1.25	1.36
		Averages	1.28	1.26

Table 5.4 Comparison of splice spacing

There is a splice spacing at which offset splices will perform significantly better than side-by-side splices. As the center-to-center spacing of the splices decreases, the difference in clear spacing of the two configurations becomes more influential in affecting splice strength.

5.5 Design Checklist

A designer can evaluate the acceptability of a splice with a series of checks regarding the splice orientation. The following are issues to be addressed when evaluating a splice's orientation.

1. A side-by-side splice has a smaller spacing between adjacent splices than other orientations, and therefore has the least bond strength. If a splice is designed assuming the clear spacing of a side-by-side orientation, no constructed splice orientation can produce

less favorable bond conditions. Any design, then, of a side-by-side splice will have sufficient bond strength, regardless of the splice orientation chosen by the contractor.

2. If the splice spacing is sufficiently large, side-splitting is not likely. Face-splitting and bar pull-out are failure modes for which splice orientation has no affect on bond strength. If either face-splitting or bar pull-out is likely, bond strength is not governed by splice orientation.

a.) Face-splitting will control bond strength if the clear spacing between splices is greater than twice the clear cover. This situation is shown for a side-by-side splice in Figure 5.6.

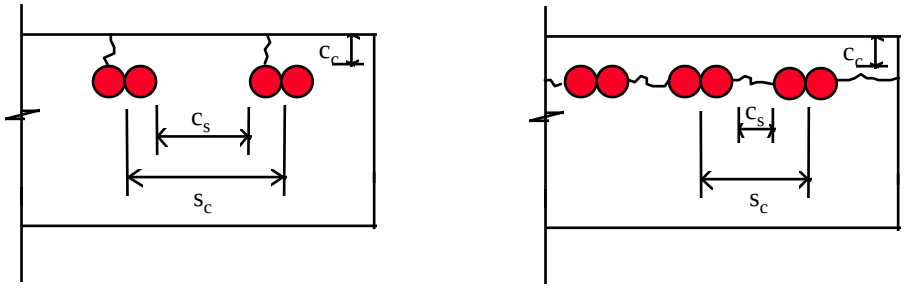

Face-splitting is likely
if $c_s > 2c_c$, or if $s_c - 2d_b > 2c_c$

Side-splitting is likely
if $c_s < 2c_c$, or if $s_c - 2d_b < 2c_c$

Figure 5.6 Failure modes as a function of clear spacing

b.) Bar pull-out is likely to control bond strength if the face cover and clear spacing between bars are both sufficiently large. In this case, $s_c - 2d_b$ may be less than $2c_c$, but side-splitting still will not occur. Orientation does not affect bond strength in the case of bar pull-out

3. The amount of transverse steel in the splice region may improve the bond enough that side-by-side splices will have adequate bond strength, even if the splice was designed assuming an offset orientation. If the amount of transverse steel is determined to be sufficient to offset the reduction in bond due to close spacing, side-by-side splices could be used without adjusting the splice length.

4. If the splice is constructed in an offset configuration, it will have at least the bond strength anticipated, regardless of which splice orientation is assumed in design.

The above alterations can be used to determine the acceptability of a constructed side-by-side splice. If none of those conditions are met, a designer has two options to ensure adequate performance of the splice:

a.) redesign the splice assuming a side-by-side configuration, or

b.) specify offset splices on drawings and monitor construction.

Figure 5.7 is a checklist to aid in evaluating the acceptability of a splice orientation.

5.6 Comparison of Test Results with ACI and AASHTO Code Provisions

To put test results into a more practical context, a comparison is made between the actual bar stresses at failure and those predicted by equations in the ACI and AASHTO specifications. The applicable code equations are all arranged to calculate a minimum splice length from the yield stress of the steel and other, known parameters. Since the splice length in each test was known, though, the equations can be reversed to calculate a bar stress at failure.

The AASHTO equations for required splice length (Equations 2.13 and 2.14), modified to calculate bar stress at failure, are:

$$f_s = \frac{l_s \sqrt{f'_c}}{1..25 A_b F_{mod}} \times \frac{1}{F_{class}}$$

but not greater than

$$f_s = \frac{l_s}{0.4 d_b l_s F_{mod}} \times \frac{1}{F_{class}}$$

where: l_s = required length of splice, in.

A_b = cross-sectional area of each bar being spliced, in^2

f_y = yield stress of the spliced steel, ksi

f'_c = concrete compressive strength, ksi

F_{mod} = modification factors based on member geometry and material properties.

F_{class} = modification factor based on the class of splice.

Likewise, the ACI equations for required splice length (equations 2.8 - 2.12) can be rearranged to compute bar stress at failure.

A summary of all actual and specification-derived bar stresses is presented in Table 5.5. The predictions from the specification equations were consistently conservative, as seen in the table. On the average, the simplified ACI equation was the most conservative, while the more accurate ACI equation was the least conservative. The margin of safety for the AASHTO equation lies between those of the two ACI equations.

Test	u_{test} MPa (ksi)	u_{AASHTO} MPa (ksi)	$u_{ACI\ (1)}$ MPa (ksi)	$u_{ACI\ (2)}$ MPa (ksi)
12-S-P	187 (27.2)	76 (11.0)	114 (16.6)	100 (14.5)
9-S-P	216(31.4)	151 (21.9)	114 (16.6)	138 (20.0)
12-O-P	239 (34.7)	162 (23.5)	134 (19.4)	192 (27.8)
9-O-P	245 (35.5)	162 (23.5)	134 (19.4)	236 (34.3)
12-S-A	198 (28.8)	81 (11.8)	93 (13.5)	85 (12.4)
9-S-A	265 (38.4)	162 (23.5)	140 (20.3)	132 (19.1)
12-O-A	271 (39.4)	155 (22.5)	118 (17.1)	127 (18.5)
9-O-A	302 (43.9)	155 (22.5)	118 (17.1)	167 (24.3)
	Margins of Safety	1.8	2.0	1.8

Table 5.5 Comparison of bar stress at failure for different code equations

CHAPTER SIX

In Which the Study is Summarized

and Conclusions are Drawn

6.1 Summary

The primary objective of this project is to evaluate the strengths of different splice orientations, side-by-side and offset, as a function of spacing between splices and the presence of transverse reinforcement. To obtain the data necessary to draw conclusions, eight tests were conducted. Three parameters were varied between tests: splice configuration, splice spacing, and the presence (or absence thereof) of transverse reinforcement in the splice region. Each of the eight tests involved a unique combination of the three variable parameters. Thus, by comparing different pairs of tests, the effects of each of the parameters on bond strength can be determined.

6.2 Conclusions

6.2.1 Splice orientation

Given the same center-to-center splice spacing, offset splices have move clear spacing between adjacent splices than do side-by-side splices. Consequently, there was a difference in the bond strength of splices of different orientations. On average, offset splices were approximately 16% stronger than side-by-side splices, consistent with predictions made using empirically derived equations. Although offset splices consistently failed at a higher stress than their side-by-side counterparts, the ratio of the two bond strengths decreased as the center-to-center spacing between splices increased. Offset splices were about 7% stronger for tests with 9 splices, while they were about 24% stronger for tests with 12 splices.

6.2.2 Presence of transverse steel

Data from the tests do not indicate that transverse reinforcement significantly contributed to bond strength. The presence of transverse steel in the splice region did offer benefits in other respects, though. The specimens lacking stirrups in the splice region failed in an abrupt manner, with the stress in the splices decreasing immediately when the peak load was reached. For specimens with stirrups in the splice region, on the other hand, the peak load was sustained with increasing deflection. At the peak load plateau, stresses were redistributed among the splices. The inclusion of transverse steel in the splice region contributed to a more ductile failure mode than was experienced in specimens with no stirrups in the splice region. The limited data and differences in materials or construction between specimens without transverse steel did not permit full evaluation of the effect of transverse reinforcement on splice strength.

6.2.3 Splice spacing

Previous tests show that increased clear cover or increased clear spacing between adjacent splices increases bond strength. In the tests conducted, splices with greater clear spacing achieved higher bond stresses. On the average, tests with 9 splices (large spacing) produced bond stresses about 26% higher than tests with 12 splices (small spacing), about as expected from previously derived equations.

6.2.4 Design considerations

For most cases, the difference in bond strength between the two splice orientations is not enough to warrant specifying one orientation or the other For some splices with little clear spacing between adjacent splices, however, the difference in bond strength is large enough that the designer should consider either specifying offset splices or recalculate the splice length assuming a side-by-side orientation.

BIBLIOGRAPHY

1. Nilson, Arthur H., and George Winter, Design of Reinforced Concrete Structures, Eleventh Edition, McGraw Hill, Inc., New York, 1991.

2. Hamad, B. S.; J. O. Jirsa; and N. L.d'Abreu d'Paolo, "Effect of Epoxy Coating on Bond and Anchorage of Reinforcement in Concrete Structures," Research Report 1181-1F, The Center for Transportation Research, The University of Texas at Austin, 1990.

3. Orangun, C. O.; J. O. Jirsa; and J. E. Breen, "The Strength of Anchored Bars: A Reevaluation of Test Data on Development Length and Splices," Research Report 154-3F, The Center for Highway Research, The University of Texas at Austin, 1975.

4. ACI Committee 318, "Building Code Requirements for Reinforced Concrete and Commentary," ACI Standard 318-89, American Concrete Institute, Detroit, Michigan, 1989

5. ACI Committe 318, "Proposed Revisions to Building Code Requirements for Reinforced Concrete (ACI 318-89) (Revised 1992) and Commentary - ACI 318R-89 (Revised 1992)," *Concrete International*, December 1994.

6. American Association of State Highway and Transportation Officials, "Standard Specifications for Highway Bridges," 1989.

7. Thompson, M. A., and J. O. Jirsa, "The Behavior of Multiple Lap Splices in Wide Sections," Research Report 154-1, The Center for Highway Research, The University of Texas at Austin, 1975.